Astron. Astrophys. 337, 940–944 (1998)

ASTRONOMY AND ASTROPHYSICS

An analytic solar magnetic field model

M. Banaszkiewicz[1], **W.I. Axford**[2], **and J.F. McKenzie**[2]

[1] Space Research Center, Polish Academy of Sciences, Bartycka 18a, PL-00716 Warsaw, Poland
[2] Max-Planck-Institut für Aeronomie, Postfach 20, D-37189 Katlenburg-Lindau, Germany

Received 23 January 1998 / Accepted 30 June 1998

Abstract. We describe a simple analytic model for the magnetic field in the solar corona and interplanetary space which is appropriate to solar minimum conditions. The model combines an azimuthal current sheet in the equatorial plane with an axisymmetric multipole field representing the internal magnetic field of the Sun. The radial component of the field filling interplanetary space is approximately monopolar at large heliocentric distances as observed. These open field lines connect to the polar regions of the Sun and define the polar coronal holes which are prevalent at solar minimum and which are the source of the fast solar wind. By including both dipole and a quadrupole terms at the origin it is possible to construct a good representation of the coronal magnetic field in such conditions. We also note that the Parker spiral will be underwound relative to the case of the monopole because the open field lines emanate from solar latitudes in excess of $60°$.

Key words: Sun: corona – Sun: magnetic fields

1. Introduction

Immediately following the Pioneer 10 encounter with Jupiter, Gleeson & Axford (1974), (1976) constructed a very simple magnetic field model involving a dipole and an azimuthal current sheet. The model describes rather well the magnetosphere of a rapidly-rotating planet containing cold, co-rotating plasma and is also applicable to the magnetic field of the solar corona and its extension into interplanetary space. Its simplicity arises from the fact that it is possible to choose forms for the current distribution which permit analytic expressions to be derived for the associated magnetic field. In particular one may choose the ratio of the dipole moments of the current sheet and of the internal planetary field to create a thin disc-like region of closed magnetic field lines equivalent to the “coronal streamer belt”. This region extends to infinity around the equatorial plane and is contained above and below by oppositely-directed fields which are ‘monopolar’ at large distances from the planet. Such a “dipole plus current sheet” (DCS) model configuration is shown in Fig. 1, which also shows the trajectory of a proposed solar probe mission [Axford et al. (1995)].

Send offprint requests to: W.I. Axford

Since the solar magnetic field observed during eclipses in sunspot minimum conditions is similar in form to such a rotating magnetosphere [Gold (1958)] and we know that the interplanetary magnetic field is dominated by a single, near-equatorial current sheet at such times, it seems appropriate to use the DCS magnetic field model also in these circumstances [Axford & McKenzie (1997)]. The monopolar behaviour of the magnitude of the radial component of the field observed at large heliocentric distances (i.e. $r^2 B_r \sim const$, [Forsyth et al. (1996)]) confirms this view and indeed is unsurprising (e.g. Schatten (1971)). Furthermore, since the open magnetic field regions, together with their associated fast solar wind, appear to connect to the polar coronal holes which persist for many years around sunspot minimum, it is obvious that the magnetic field strength in these coronal holes can be determined by magnetic flux conservation. Thus the average radial field of $\sim 3.1 \cdot 10^{-5}$ gauss at 1 a.u. measured by Ulysses [Forsyth et al. (1995)] corresponds to an average magnetic field strength of ~ 10 gauss at the base of the corona assuming the boundary of the polar coronal holes to be at 60 degrees solar latitude (e.g. Axford (1976); Gabriel (1976)). (In making this estimate the magnetic flux contained in the slow wind belt near the equatorial plane is excluded as this should not connect to the polar coronal holes.)

There are however some drawbacks of the DCS model as described. If it is assumed that plasma on closed field lines forms the near-Sun coronal streamer belt and that the open field lines contain lower-density, fast solar wind (apart from discrete polar plumes) then the shape of the field lines in the polar regions does not appear to be correct. Coronagraph observations [Habbal et al. ,1995]; [Schwenn, private communication ,1996] suggest that the polar plumes, and therefore the magnetic field lines in the polar corona, are almost straight beyond about $1.5R_S$. Furthermore, the high-latitude boundary of the streamer belt does not appear to bulge nearly as much above the equatorial plane as does the last closed field line shown in Fig. 1. The DCS model suggests that the view from the Earth of the (low density) polar corona below about $3R_S$ heliocentric distance is likely to be obscured by higher density regions associated with coronal streamers in the line-of-sight from the Earth, which is certainly not always so (e.g. Loucif & Koutchmy (1989); L. Strachan, private communication (1996)). We can adjust the strength of

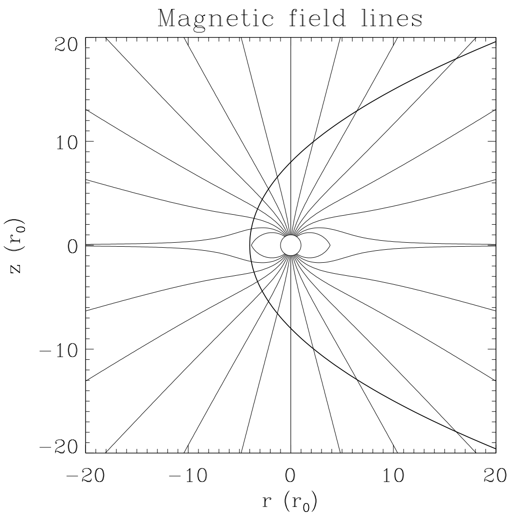

Fig. 1. The magnetic field lines for the DCS model with the last closed field line intersecting the surface of the Sun at 60 degrees latitude. The parabola indicates the possible trajectory of a Solar Probe mission with a perihelion distance of $4 \cdot R_S$. The magnetic field lines are essentially monopolar beyond about $10 \cdot R_S$ except in the streamer belt. Close to the Sun the field lines are sufficiently non-radial to cause a potential plasma viewing problem for the mission.

the current sheet to correct these deficiencies to some extent but it appears to be more appropriate to modify the solar field.

2. The dipole plus quadrupole plus current sheet (DQCS) model

The DCS model can be improved by the inclusion of a quadrupole component of the internal field of the Sun, as suggested for example by Brueckner et al. (1996). The corresponding components of the magnetic field in this case (the DQCS model) are given analytically (in gauss) in cylindrical polar coordinates (ρ, z in solar radii) as follows:

$$\frac{B_\rho}{M} = \frac{3\rho z}{r^5} + \frac{15Q}{8}\frac{\rho z}{r^7}\frac{(4z^2 - 3\rho^2)}{r^2} + \frac{K}{a_1}\frac{\rho}{[(|z| + a_1)^2 + \rho^2]^{3/2}}, \tag{1}$$

$$\frac{B_z}{M} = \frac{2z^2 - \rho^2}{r^5} + \frac{3Q}{8}\frac{(8z^4 + 3\rho^4 - 24\rho^2 z^2)}{r^9} + \frac{K}{a_1}\frac{|z| + a_1}{[(|z| + a_1)^2 + \rho^2]^{3/2}}, \tag{2}$$

where $r^2 = \rho^2 + z^2$ and $Q = 0$ corresponds to the DCS model. In order to make the last closed field line (which extends to large distances) intersect the Sun at 60 degrees latitude, and to have $B_r \sim 3.1 \cdot nT$ at 1 a.u., it is necessary to choose $K = 1.0$, $M = 1.789$ and $a_1 = 1.538$ in the limiting case $Q = 1.5$ where all field lines still connect with the Sun. (As before we make an allowance for the magnetic flux contained in the slow wind belt.) The evolution of the field configuration as Q is increased from zero to > 1.5 is shown in Fig. 2 and an expanded version of the case $Q = 1.5$ in Fig. 3. It should be noted that for $Q > 1.5$ there are field lines surrounding the current sheet which do not connect with the Sun and which, under steady conditions, are unphysical although they may be suggestive of what happens when the field changes or reconnects.

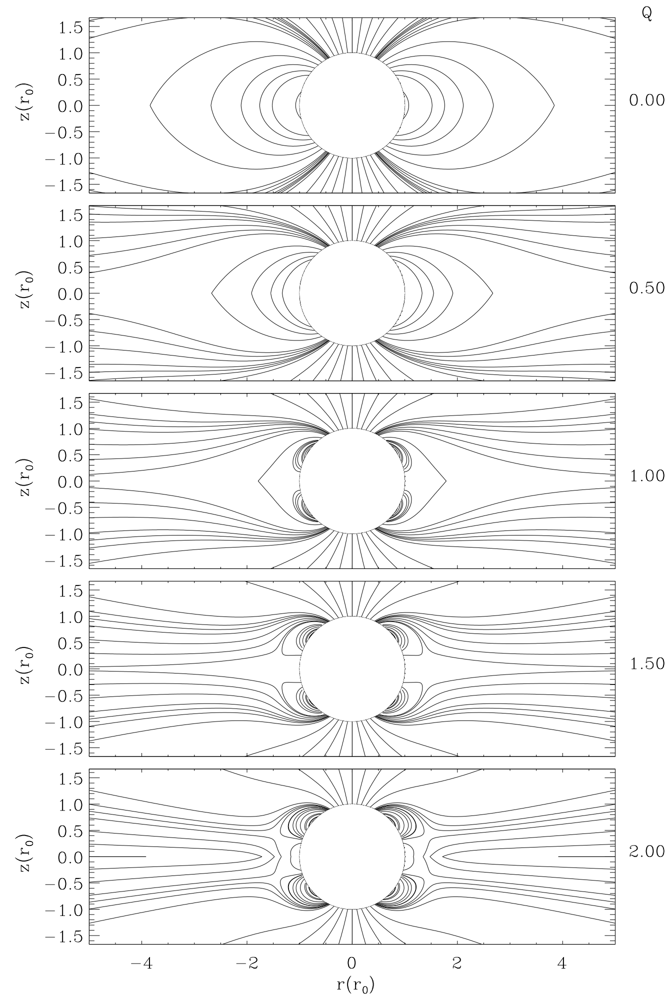

Fig. 2. The evolution of the magnetic field configuration for the DQCS model with increasing values of Q. The case $Q = 0$ is the DCS model shown in Fig. 1. The effects of the quadrupole become more pronounced as Q increases until $Q = 1.5$ when there is a direct link from the solar equator to infinity along the equatorial plane and current sheet. For $Q > 1.5$ there is a neutral point close to the Sun in the equatorial plane with detached field lines at larger distances; this is unphysical although suggestive of what could happen as a result of reconnection in the corona. Note that the close spacing of the field lines shown, especially in the quadrupole loops, does not represent the field strength but is simply intended to provide better detail where needed.

The model can easily be compared with observations. First, it predicts the monopolar behaviour of the radial component of the field at large distances observed by Ulysses. Second, ultraviolet images of the polar corona (SUMER and EIT on SOHO) and coronagraph observations (LASCO C1 and UVCS on SOHO) provide information on the direction of the field lines in the po-

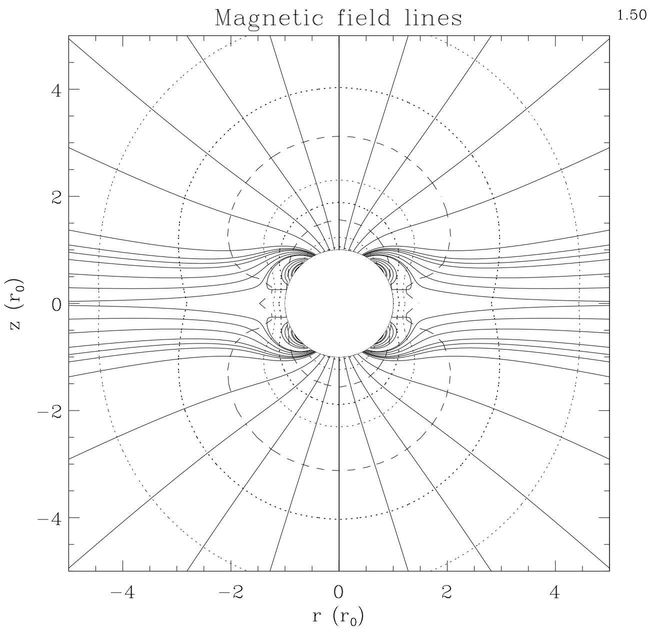

Fig. 3. An enlarged version of the DQCS model for the limiting case $Q = 1.5$. On comparing with Fig. 1 it is evident that the potential plasma viewing problem for a Solar Probe mission has diminished since the field lines are essentially straight although not radial everywhere along the trajectory. The dashed lines indicate surfaces of constant field strength.

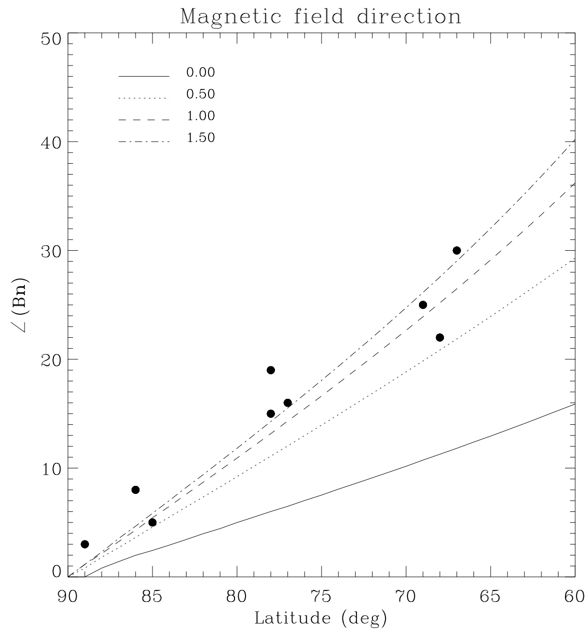

Fig. 4. The direction of the magnetic field at the limb in polar coronal holes determined by measuring the angle between the radial direction and wisps of UV emission which are presumed to indicate the direction of the field. The measurements are not consistent with the DCS model ($Q = 0$) and if anything are best represented by the limiting case $Q = 1.5$.

lar regions which can be compared directly with the models. In particular, the short wisps of emission observed at the limb by SUMER and EIT give the field directions at the base of the corona: we have measured the angles relative to the radial direction using SUMER images (Fig. 4) and find that the case $Q = 1.5$ fits rather well whereas $Q = 0$ is certainly excluded. Furthermore, the essentially straight field lines observed beyond $\sim 1.5R_S$ are easily reproduced in the case $Q = 1.5$, although it is important to note that these field lines are not radial but converge near the poles. There are immediate and useful implications of the above for solar wind modelling. The fast wind can be assumed to flow along the field lines and the field strength therefore controls its divergence. In particular, along the straight polar field line,

$$\frac{B}{M} = \frac{2}{r^3} + \frac{3Q}{r^5} + \frac{K}{a_1(r+a_1)^2} \tag{3}$$

One can immediately see from this result that the current sheet determines the monopolar form of the field at large distances from the Sun. The field strength at the base of the polar coronal hole is dominated by the dipole and quadrupole components, being 11.8 gauss at the pole and falling to 7.8 gauss at the edge at 60 degrees latitude (see Fig. 5). Similarly the local expansion factor f, which we define as the ratio of the field strength at the base of the corona to that of a monopole with the same field at large distances ($MK/a_1 = 1.29$), is ~ 10 at the pole and ~ 6.7 at the edge. (Note that the form of the expansion, which is determined by B, is rapid and not uniform across the polar cap. Furthermore, the direction of the field in the photosphere is not necessarily the same as at the base of the corona.)

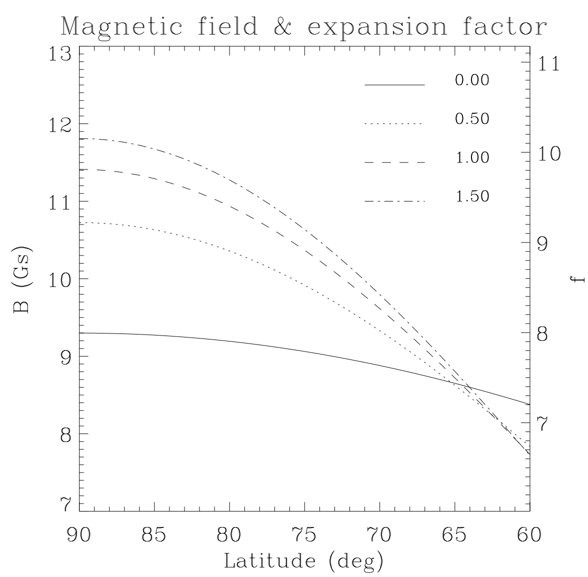

Fig. 5. The variation of surface field strength B and Br, and the local expansion factor f within the polar coronal hole (latitudes > 60 degrees) for various values of Q.

The fact that the inclusion of the quadrupole term weakens the solar magnetic field around the equator is interesting from the point of view of the origin of the slow solar wind. In the limiting case $Q = 1.5$, there is a direct connection from the Sun to infinity along the equatorial plane where $B = 0$ everywhere. LASCO C1 observations of persistent but fluctuating dense plasma emission from the equatorial regions suggest that this might indeed be the source region of the slow wind [Schwenn, private communication (1996)]. It has long been understood that, in contrast with the fast wind, the slow wind is essentially transient and filamentary and not in equilibrium with its coronal base [Axford (1977)] so that this region is in many respects well-suited to produce the necessary environment for the source of the slow wind. We emphasise however that our model is a simple one, primarily designed to provide a simple field description for polar coronal holes, and it should not be over-interpreted.

3. Modification of the Parker spiral

In our DQCS model of the magnetic field the Parker spiral angle is modified to reflect the fact that the open field lines emanate from solar latitudes $\theta_S \geq 60°$, with the result that the field observed at large distances will appear underwound because the rotation rate decreases with solar latitude. We can quantify this effect as follows. The rotation rate of the photosphere $\Omega(\theta_S)$ is given approximately by [Howard & Harvey (1970)]

$$\Omega(\theta_S) = \frac{1}{26}(1 - \frac{1}{8}\sin^2\theta_S - \frac{1}{6}\sin^4\theta_S) \quad rotations/day. \quad (4)$$

The relation between θ_S and the latitude θ to which the field line is asymptotic may be obtained from the field line equation which is given by the ϕ component of the vector potential A_ϕ, namely

$$\rho A_\phi(r_S, \theta_S) = \rho A_\phi(r \to \infty, \theta) \quad (5a)$$

where

$$\rho A_\phi(r,\theta) = M\left\{\frac{\rho^2}{r^3} + \frac{3\rho^2 Q}{8r^5}(4 - \frac{5\rho^2}{r^2}) + \frac{K_1}{a_1}\left[1 - \frac{|z| + a_1}{((|z| + a_1)^2 + \rho^2)^{1/2}}\right]\right\}. \quad (5b)$$

$\rho = r\cos\theta$, $z = r\sin\theta$.

As $r \to \infty$, $\rho A_\phi \to (K_1/a_1)(1 - |\sin\theta|)$. Therefore the relation between θ and θ_S (for $\theta \geq 0$) is given by

$$\sin\theta = 1 - \frac{a_1}{K_1}\left[\frac{\cos^2\theta_S}{r_S} + \frac{3}{8}Q\frac{\cos^2\theta_S}{r_S^2}(4 - 5\cos^4\theta_S)\right] + \frac{K_1}{a_1}\left[1 - \frac{r_S\sin\theta_S + a_1}{((r_S\sin\theta_S + a_1)^2 + r_S^2\cos^2\theta_S)^{1/2}}\right]. \quad (6)$$

Fig. 6 shows θ_S as a function θ for various values of the quadrupole moment Q. This fanning out of the field lines is to a good approximation described by $\theta_S - 60° \approx \theta/3$. We have used this to construct Fig. 7 which shows the ratio of the rotation rate as function of θ to the rotation rate of a monopole. This shows that the Parker spiral can be as much as 20% underwound at the equatorial current sheet, 10% underwound at $\theta = 60°$ and of course "correctly" wound over the poles. Ulysses observations of the heliospheric magnetic field [Forsyth et al., 1996] appear to support this trend of underwinding. Further evidence of this effect is provided by Smith et al. (1997) who plot Ulysses measurements of the ratio $< rVB_T > /\Omega_0 < r^2 B_r >$ as a function of the sine of the colatitude. Here Ω_0 is the equatorial rotation rate, V is the solar wind speed and B_T and B_r are respectively the azimuthal and radial components of the magnetic field given by [e.g. Parker (1963)],

$$(B_r, B_T) = B_0 r_0^2\left(\frac{1}{r^2}, \frac{\Omega\sin\phi}{rV}\right), \quad (7)$$

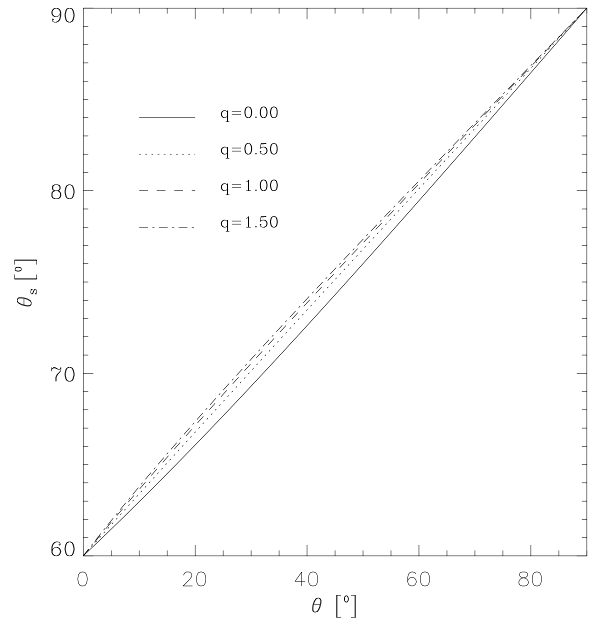

Fig. 6. Solar latitude θ_S as a function of "asymptotic" latitude θ for various values of the quadrupole moment Q.

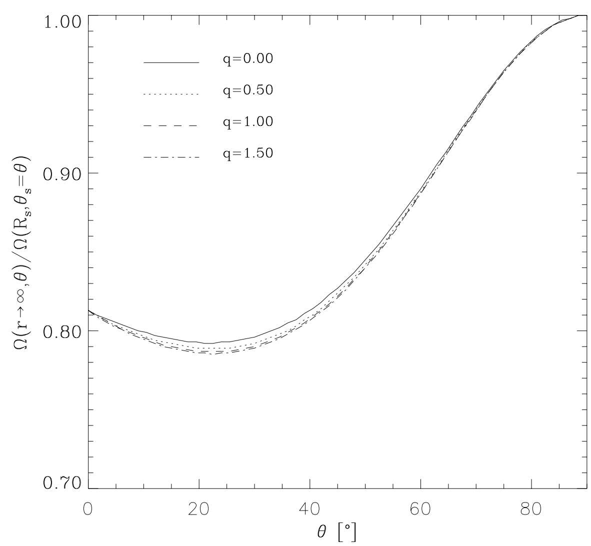

Fig. 7. The ratio of the rotation rate as function of θ to the rotation rate of a monopole.

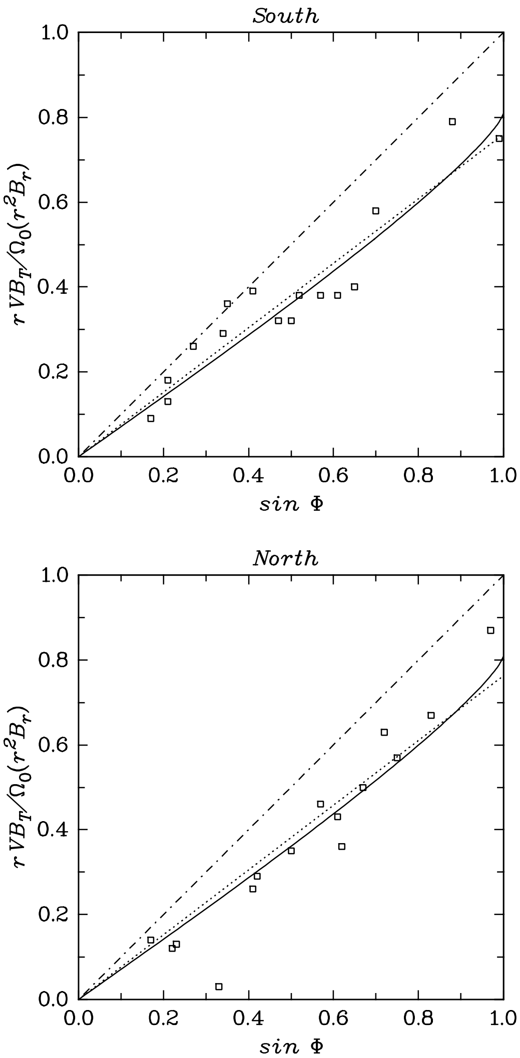

Fig. 8. The solid curve $(\Omega/\Omega_0)\sin\phi$ is in good agreement with the Ulysses observations (squares) and their best fit line [Smith et al., 1997]. (The dash-dot line corresponds to solid body rotation.)

where ϕ is the co-latitude ($\phi = \pi/2 - \theta$). Hence we have

$$\frac{rVB_T}{\Omega_0 r^2 B_r} = \frac{\Omega}{\Omega_0}\sin\phi. \tag{8}$$

Using Eq. (4)for the rotation rate and the approximate relation $\theta_S = \theta/3 + \pi/3$ which describes how the field lines fan out from solar latitudes in excess of 60° we have plotted $(\Omega/\Omega_0)\sin\phi$ as a function of $\sin\phi$. It will be observed from Fig. (8) that this curve provides a remarkably good fit to the observations, indicated by the squares, and the best line (the dotted line), in both hemispheres. Note that this result is independent of the inclusion of a quadrupole moment whose main influence is felt close to the Sun. However since the observed parameters plotted in Fig. 8 are mean values of an asymmetric distributions (see Smith et al. (1997) for futher discussion) and also because we have neglected the small tilt of the dipole, physical conclusions based on the agreement with the model with these observations should be treated with some caution.

4. Conclusions

The DQCS solar magnetic field model described here appears to provide a sound and useful basis for further studies, especially of the flow of the fast solar wind which dominates interplanetary space during solar minimum conditions. Since it involves only an axisymmetric dipole and quadrupole and specific forms for the current sheet, it is of course not a substitute for more detailed models with more complex surface conditions and force-free fields, where these are needed. In particular, the current sheet may be regarded as being only a proxy for the effects of plasma pressure in the closed field region and also of rotation since it does not describe the physics involved. Nevertheless the model must provide a good representation of the structure of the magnetic field in a well- developed polar coronal hole and indeed appears to fit observations of the field directions implied by wisps of UV emission at the limb and by rays which extend to several solar radii in the polar regions. We also note that since the open field lines in our DQCS model emanate from solar latitudes greater than 60 degrees the Parker spiral at large distances will appear underwound relative to that expected from a monopole.

Acknowledgements. We thank the MPAE/SUMER group for providing the images used to construct Fig. 4, and the referee for constructive comments.

References

Axford W. I., 1976, in: Physics of Solar Planetary Environments, ed. D.Williams, Am. Geophys. Union, 145

Axford W. I., 1977, in: Study of Travelling Interplanetary Phenomena, eds. M.A.Shea, D.F.Smart and S.-T. Wu,D.Reidel, Dordrecht, 149-164

Axford W.I. et al., 1995, Report of the Minimum Solar Mission Science Team, JPL

Axford W. I., McKenzie J. F., 1997, in: Cosmic Winds, University of Arizona Press, Tucson, 31-66

Brueckner G. et al., 1996, Advances in Space Research, in press

Forsyth R.J. et al., 1996, A&A 316, 287

Gabriel A., 1976, Phil.Trans.Roy.Soc., A28, 339

Glesson L.J, Axford W.I., 1974, Eos, Trans. AGU, 55, 404

Glesson L.J, Axford W.I., 1974, J. Geophys. Res., 81, 3403

Gold T., 1958, in: Electrodynamic Phenomena in Cosmical Physics, ed. B.Lehnert, IAU Symposium 6, 275

Habbal S.R., 1995, Geophys.Res. Lett., 22, 1465

Howard R., Harvey J., 1970, Solar Phys. , 12, 23

Loucif M.L., Koutchmy S. 1989, Astron. Astrophys. Suppl. Ser., 77, 45

Parker E.N., 1963, Interplanetary Dynamical Processes, Wiley-Interscience, New York

Schatten K.A., 1971, Cosmic Electrodynamics, 2, 232

Smith E.J. et al., 1997, Adv. Space Res., 20, 1